JTTEE5 20:132–138
DOI: 10.1007/s11666-010-9601-1
1059-9630/$19.00 © ASM International

The Oxidation Behavior of TBC with Cold Spray CoNiCrAlY Bond Coat

W.R. Chen, E. Irissou, X. Wu, J.-G. Legoux, and B.R. Marple

(Submitted June 30, 2010; in revised form October 25, 2010)

Cold gas dynamic spray (CGDS) has been considered a potential technique to produce the metallic bond coat for TBC applications, because of its fast deposition rate and low deposition temperature. This article presents the influence of spray processes for bond coat, including air plasma spray, high velocity oxy-fuel, and in particular CGDS, on the oxidation performance of TBCs with a Co-32Ni-21Cr-8Al-0.5Y (wt.%) bond coat and an air plasma sprayed topcoat. Oxidation behavior of the TBCs was evaluated by examining the coating microstructural evolution, TGO growth behavior, and crack propagation during thermal exposure at 1050 °C. The relationship between the TGO growth and crack propagation will be discussed.

Keywords cold spray, CoNiCrAlY, cracking, oxidation, TBC, TGO growth, thermal spray

1. Introduction

In a thermal barrier coating (TBC) system, the metallic bond coat (BC) plays the role of enhancing the adhesion of the ceramic topcoat (TC) to the substrate and protecting the substrate metal from oxidation and corrosion. When exposed at high temperatures, oxidation of the bond coat results in the formation of a thermally grown oxide (TGO) layer at the ceramic/bond coat interface. This layer acts as a diffusion barrier during the extended thermal exposure in service, thus protecting the substrate from further oxidation. However, growth of the TGO tends to increase the internal stress within the TBC system and causes cracking in the TC/BC interfacial region, which eventually leads to spallation of the topcoat (Ref 1-5).

In previous studies on TBCs with thermal spray bond coats, it was found that the growth of the TGO layer first proceeded in a parabolic manner with time, which was then followed by an accelerated growth stage (Ref 6-9). It was shown that TGO growth was dependent on the thermal spray processes (Ref 8). A power-law relationship between the maximum crack length and TGO thickness was observed in recent studies (Ref 9-11).

In recent years, cold gas dynamic spray (CGDS) deposition of metallic bond coats has been studied (Ref 12-20). CGDS utilizes a supersonic gas jet to accelerate fine solid powders above a critical velocity at which particles impact, deform plastically, and bond to the substrate material in the ambient environment. This process is potentially beneficial for TBC bond coat deposition because it would avoid oxidation of the feedstock powder that normally occurs when higher temperature thermal spray processes are employed. Therefore, there would be no prior aluminum depletion in as-deposited bond coats produced by the CGDS technique. This study investigates the influence of various bond coat deposition processes, including air plasma spray (APS), high velocity oxy-fuel (HVOF), and, in particular, CGDS, on the oxidation performance of TBCs with a Co-32Ni-21Cr-8Al-0.5Y (wt.%) bond coat and an air plasma sprayed topcoat.

2. Experimental

The TBCs consisted of a CoNiCrAlY bond coat and a ZrO_2-8wt.%Y_2O_3 topcoat. The bond coat was deposited to a thickness of 140-180 μm by the APS, HVOF, or CGDS technique with powders of Co-32Ni-21Cr-8Al-0.5Y (wt.%), onto ∅16 × 10 mm Inconel 625 disks. On top of the CoNiCrAlY, the topcoat was deposited to a thickness of 250-280 μm by the APS technique, with powders of ZrO_2-8wt.%Y_2O_3. The spray techniques and feedstock are described in Table 1, whereas spraying conditions are shown in Table 2. Both BC and TC were produced based on the spray parameters recommended by the manufacturers of the torch and feedstock except for the CGDS BC for which the spray parameters where adjusted to attain a compromise between the faster particle velocity using nitrogen as propelling gas and preventing clogging of the

This article is an invited paper selected from presentations at the 2010 International Thermal Spray Conference and has been expanded from the original presentation. It is simultaneously published in *Thermal Spray: Global Solutions for Future Applications, Proceedings of the 2010 International Thermal Spray Conference*, Singapore, May 3-5, 2010, Basil R. Marple, Arvind Agarwal, Margaret M. Hyland, Yuk-Chiu Lau, Chang-Jiu Li, Rogerio S. Lima, and Ghislain Montavon, Ed., ASM International, Materials Park, OH, 2011.

W.R. Chen and **X. Wu**, NRC-IAR-SMPL, 1200 Montreal Road, Ottawa, ON K1A 0R6, Canada; and **E. Irissou, J.-G. Legoux,** and **B.R. Marple**, NRC-IMI, 75, de Mortagne, Boucherville, QC J4B 6Y4, Canada. Contact e-mail: weijie.chen@nrc-cnrc.gc.ca.

Table 1 Spraying techniques and feedstock

Spray torch		Feedstock	
Technique	**Torch manufacturer**	**Powder manufacturer**	**Nominal particle size, μm**
Bond coat			
APS	F4-MB, Sulzer Metco Westbury, NY, USA	Amdry 9951, Sulzer Metco Westbury, NY, USA	5-37
HVOF	Tafa JP5000, Praxair CT, USA	CO-210-24, Praxair CT, USA	20-45
CGDS	KINETIKS® 4000, CGT GmbH Ampfing, Germany	Amdry 9951, Sulzer Metco Westbury, NY, USA	5-37
Topcoat			
APS	F4-MB, Sulzer Metco Westbury, NY, USA	Metco 204NS, Sulzer Metco Westbury, NY, USA	11-125

Table 2 Spraying conditions

Bond coat	
APS	
Spray torch	Sulzer Metco F4-MB
Flow rate	Primary gas: Argon (65 L/min) Secondary gas: hydrogen (8 L/min) Carrier gas: argon (2 L/min)
Current	650 A
Voltage	59.3 V
Distance between the torch exit and substrate	14.5 cm
HVOF	
Spray torch	Praxair Tafa JP5000
Flow rate	Kerosene: 22.7 L/h Oxygen: 1007 L/min Carrier gas: nitrogen (9 L/min)
Barrel length	10.2 cm
Distance between the torch exit and substrate	25.4 cm
CGDS	
Spray torch	CGT Kinetiks 4000
Flow rate	Nitrogen, 40 bar, 80 m^3/h
Substrate temperature	700 °C
Distance between the torch exit and substrate	4 cm
Topcoat	
APS	
Spray torch	Sulzer Metco F4-MB
Flow rate	Primary gas: argon (35 L/min) Secondary gas: hydrogen (12 L/min) Carrier gas: argon (2.6 L/min)
Current	600 A
Voltage	61 V
Distance between the torch exit and substrate	12 cm

MOC24 nozzle because of a too high gas temperature. The inlet gas pressure and temperature were thus 40 bar and 700 °C, respectively. This CGDS process was not an optimized process. No heat treatment was applied to the TBCs prior to thermal exposure.

All TBC specimens were subjected to thermal cycling in air, which consisted of 10-15 min ramping, 100 h holding at 1050 °C, and >40 min cooling to the ambient temperature (25 °C). The oxidized samples were sectioned after completion of a predetermined number of thermal cycles that resulted in thermal exposure times between 100 and 5000 h. The cross sections were mounted using epoxy and mechanically polished. The specimens were then examined using a Philips XL30S FEG scanning electron microscope (SEM) with an energy-dispersive spectrometer (EDS). The area and length of TGO, as well as the crack length in the TBC, were measured using ImageTool software, based on the micrographs taken from the cross sections of the tested samples. The TGO area was measured by drawing a polygon along the ceramic/TGO and TGO/bond coat interfaces, while the TGO length was determined by drawing a line as short as possible along the TGO. From each specimen, 20-70 micrographs were taken for the TGO measurement. The various oxides were identified by SEM-EDS.

3. Results and Discussion

3.1 Coating Microstructures

The ceramic topcoats on all the TBC specimens were uniformly deposited using the APS technique. The typical topcoat microstructure contained porosity and splat boundaries, which present as crack-like discontinuities (Fig. 1). The maximum dimension of the crack-like discontinuities in the ceramic topcoat was in the range of 70-100 μm. The as-sprayed APS-CoNiCrAlY contained segmented Al_2O_3 veins (Fig. 1a) within the bond coat as well as at the TC/BC interface. A semi-quantitative SEM/EDS analysis showed that the aluminum concentration was highly nonuniform in the as-sprayed APS bond coat, with some regions having very low Al content (Table 3), compared to that in the CoNiCrAlY powder (≈16 at.%). This nonuniformity of Al distribution in the bond coat was documented in some previous researches (Ref 9), and can probably be attributed to the preferential oxidation and/or vaporization in the plasma, because the particle surface temperature was much higher than the melting point of the CoNiCrAlY.

The as-sprayed HVOF-CoNiCrAlY (Fig. 1b) was rather uniform and contained much less oxide as compared to the APS-CoNiCrAlY (Fig. 1a). A semi-quantitative SEM/EDS analysis showed that the aluminum concentration in HVOF-CoNiCrAlY at the TC/BC interface was much higher than that in APS-CoNiCrAlY (Table 2).

The as-sprayed CGDS-CoNiCrAlY (Fig. 1c), on the other hand, contained some discontinuities such as splat boundaries, due to insufficient plastic deformation during CGDS process. No oxide could be observed within the bond coat or at the TC/BC interface.

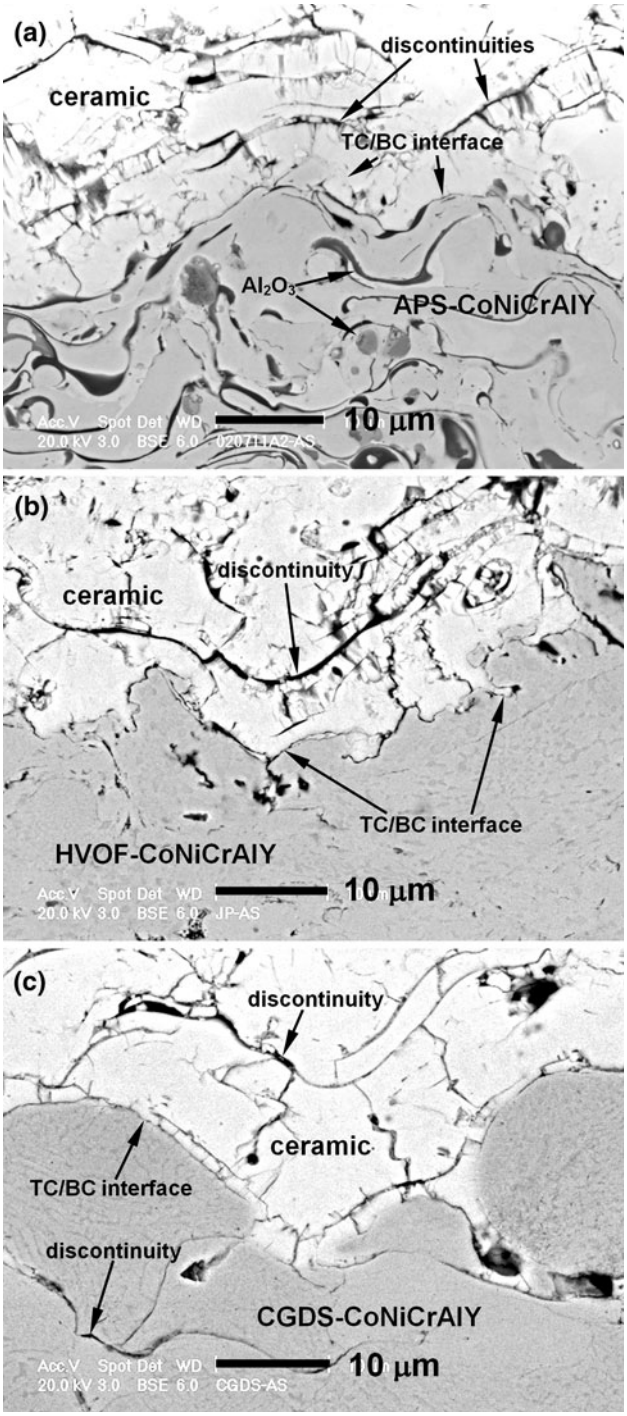

Fig. 1 Microstructures of as-sprayed (i.e., no vacuum heat treatment applied) TBCs with (a) APS- (b) HVOF-, and (c) CGDS-CoNiCrAlY bond coats

3.2 Oxidation of TBCs with CoNiCrAlYs

Upon thermal exposure in air, a layer of mixed oxides, predominantly $(Cr,Al)_2O_3 + (Co,Ni)(Cr,Al)_2O_4$ (CS), formed along the interface between the ceramic topcoat and the bond coat (Fig. 2a) in the APS-CoNiCrAlY. The Al_2O_3 portion in this oxide layer was apparently less than 20%. At the same time, clusters of chromia, spinel, and nickel oxide, abbreviated as CSN, also formed at the ceramic/bond coat interface. As such, the TGO formed in the APS-CoNiCrAlY consisted of a CS layer and CSN clusters.

As thermal exposure continued, the TGO layer grew thicker (Fig. 2b), and in the meantime, pre-existing crack-like discontinuities in the ceramic developed into fully open cracks. Extensive crack propagation in the ceramic topcoat and associated with the CSNs was also observed after 600 h (Fig. 2c). The APS-CoNiCrAlY-TBC failed after 700 h.

The TGO formed in the HVOF-CoNiCrAlY was composed of a layer of predominantly Al_2O_3 and some scattered clusters of alumina, spinel and nickel oxide (ASN) and CSNs (Fig. 3a). Opening of pre-existing discontinuities also occurred in the HVOF-CoNiCrAlY-TBC after extended thermal exposure, which led to formation of long cracks via crack propagation and coalescence in the ceramic topcoat (Fig. 3b). The TBC with HVOF-CoNiCrAlY failed after 5000 h.

Similar to the HVOF-CoNiCrAlY, CGDS-CoNiCrAlY developed a TGO that was composed of a layer of predominantly Al_2O_3, as well as some ASNs and CSNs (Fig. 4a); however, the CSNs in the CGDS-CoNiCrAlY were apparently much less than in the HVOF-CoNiCrAlY. After extended thermal exposure, opening of pre-existing discontinuities also occurred in the CGDS-CoNiCrAlY-TBC, which led to crack propagation and coalescence, forming longer cracks in the ceramic (Fig. 4b). The TBC with CGDS-CoNiCrAlY failed after 4300 h.

It was noticeable that the open discontinuity(s) between the two adjacent CoNiCrAlY particles (Fig. 5a), near the ceramic/bond coat interface in the as-sprayed CGDS-CoNiCrAlY, led to preferred oxidation along the discontinuity boundaries (Fig. 5b), due to the fast oxygen transportation along the open discontinuities. Since the CGDS process in this study was not optimized, process optimization as well as post-spraying surface treatment, such as laser ablating to obtain a dense layer in the CGDS-CoNiCrAlY next to the ceramic/bond coat interface, may be necessary to avoid such accelerated oxidation.

Table 3 Aluminum concentrations in the bond coats

Bond coat	Al, at.%
APS-CoNiCrAlY	9.6-17.9
HVOF-CoNiCrAlY	14.7-23.2
CGDS-CoNiCrAlY	15.4-20.8

3.3 TGO Growth and Crack Propagation in the TBCs

To take into account the entire TGO, an equivalent TGO thickness, δ_{eq}, is defined as (Ref 21):

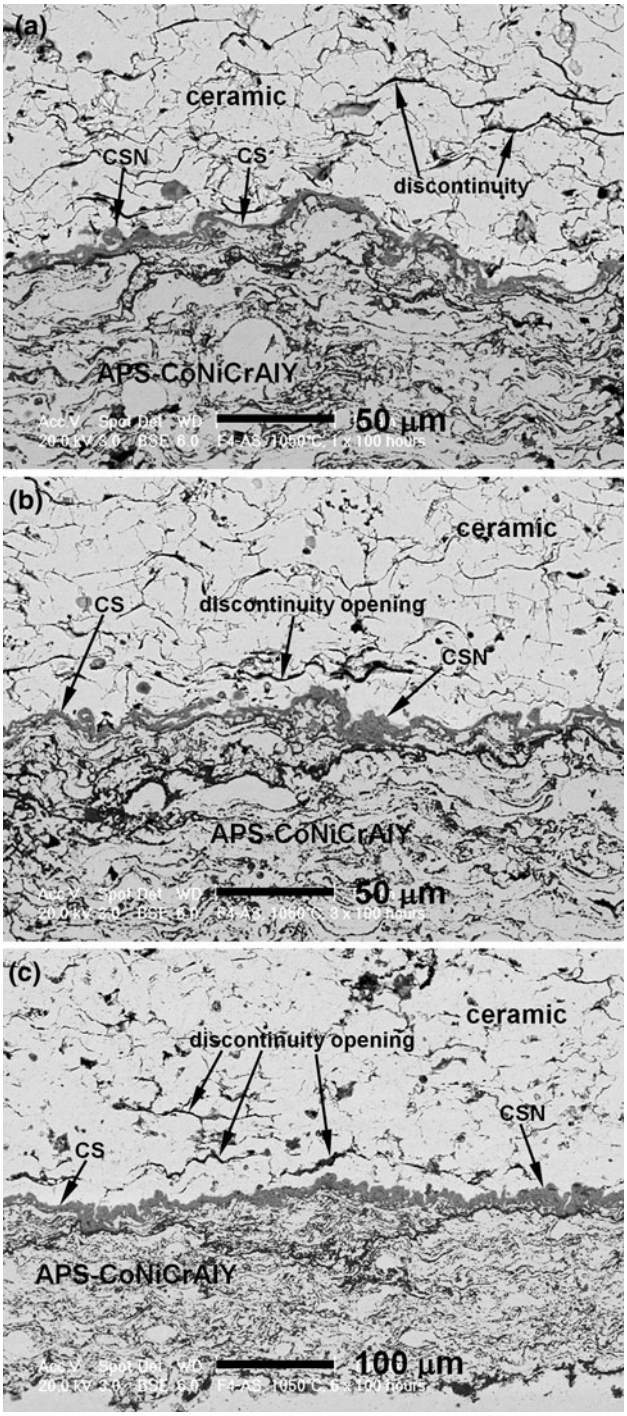

Fig. 2 As-sprayed APS-CoNiCrAlY shows (a) a TGO layer of chromia + spinel with CSNs after 100 h, (b) discontinuity opening after 300 h, and (c) crack propagation and coalescence associated with the TGO after 600 h

$$\delta_{eq} = \frac{\sum (\text{cross-sectional TGO area})}{\sum (\text{cross-sectional length of TC/BC interface})} \quad \text{(Eq 1)}$$

This approach helped to simplify the complexity arising from the rough TC/BC interface, as well as heterogeneous

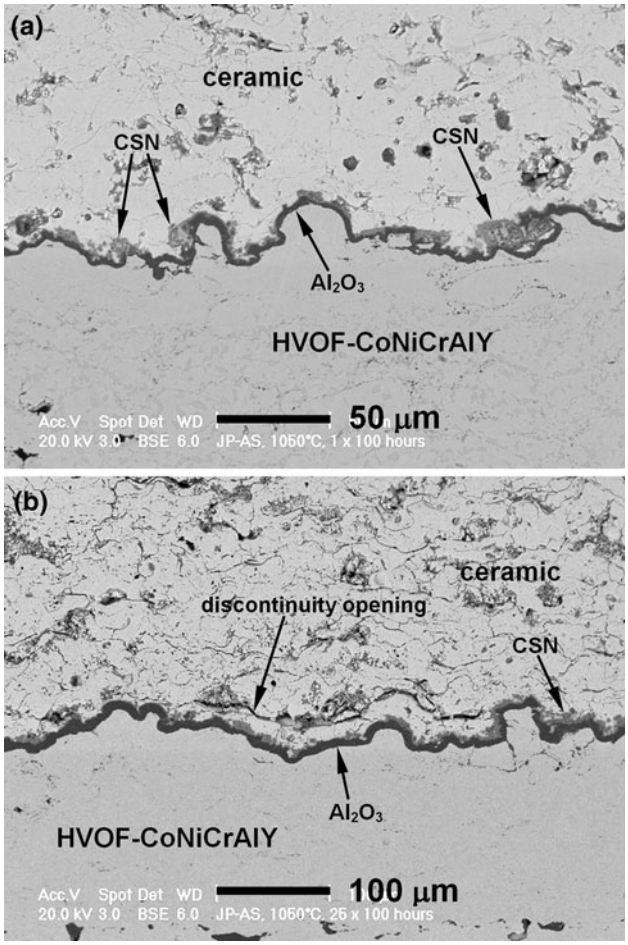

Fig. 3 As-sprayed HVOF-CoNiCrAlY shows (a) a TGO layer of predominantly alumina with ASN and CSN clusters after 100 h, (b) a discontinuity in the ceramic/bond coat interface region developed into a crack after 2500 h

TGO growth especially when ASN and CSN clusters were formed between the ceramic topcoat and the bond coat (Fig. 2-4). The relationship between δ_{eq}^2 and exposure time (Fig. 6) shows a two-stage TGO growth, i.e., an instantaneous growth followed by a parabolic growth, with HVOF- and CGDS-CoNiCrAlYs, which is consistent with some previous observations (Ref 6, 22-24), and a three-stage TGO growth with APS-CoNiCrAlY which is quite similar to that observed in a thermal cyclic test (Ref 9).

It can also be seen that both HVOF- and CGDS-CoNiCrAlYs had higher TGO growth rates than the APS-CoNiCrAlY at the very beginning of the thermal exposure; however, the latter exhibited an accelerated TGO growth after 400 h (Fig. 6), leading to TBC failure. At this point, aluminum depletion would reach a critical point such that heterogeneous oxidation would occur underneath the TGO, leading to the onset of accelerated TGO growth (Ref 9). A recent report showed a faster mass gain with the APS-CoNiCrAlY coating up to 100 h at 1000 °C (Ref 20), compared to the HVOF- and CGDS-CoNiCrAlYs.

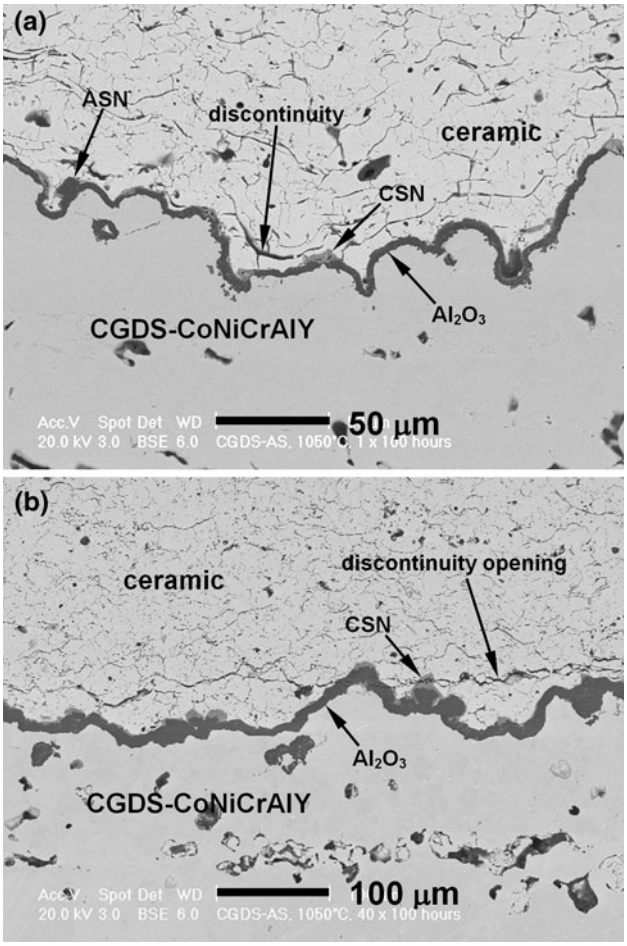

Fig. 4 As-sprayed CGDS-CoNiCrAlY shows (a) a TGO layer of predominantly alumina with ASN and CSN clusters between the ceramic topcoat and alumina layer after 100 h, (b) the increased thickness of the TGO and a discontinuity in the ceramic/bond coat interface region developed into a crack after 4000 h

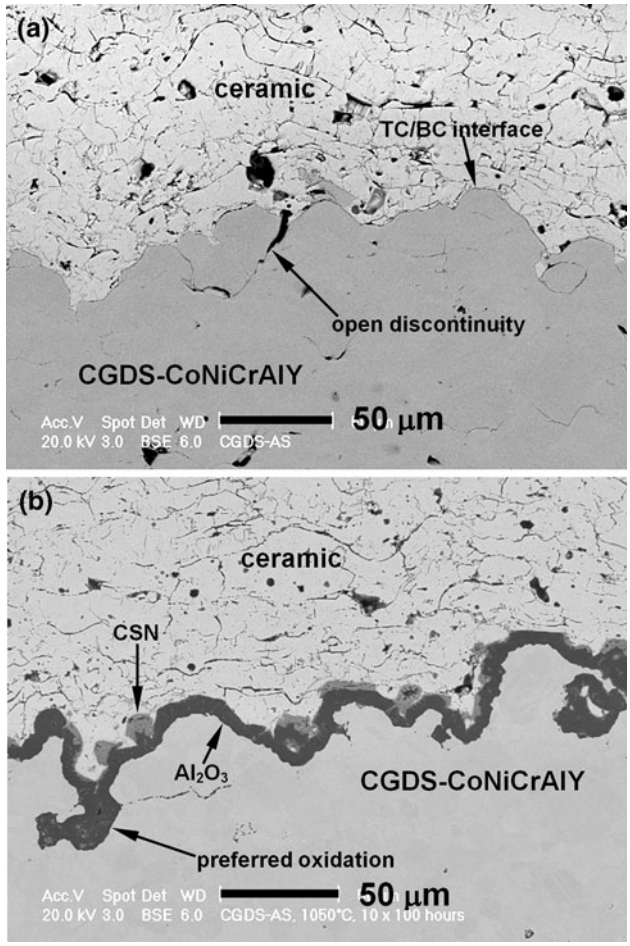

Fig. 5 As-sprayed CGDS-CoNiCrAlY shows (a) an open discontinuity between two adjacent CoNiCrAlY particles at the ceramic/bond coat interface, (b) the preferred oxidation along such open discontinuity after 1000 h

The maximum crack size a_{max} (found in all viewing sections of the coating) was chosen as the parameter to evaluate the cracking behavior in the TBCs examined. In general, the maximum crack length in a TBC increased as the exposure time increased (Fig. 7). It may be noticed that cracks propagated faster in the APS-CoNiCrAlY-TBC specimens than in the HVOF- and CGDS-CoNiCrAlY-TBCs. Plotting the maximum crack length as a function of TGO thickness (Fig. 8) reveals that $\log(a_{max})$ versus $\log(\delta_{eq})$ has a nearly linear relationship, suggesting that the relationship between the maximum crack length in the TBC and TGO thickness can be expressed by a power law relationship:

$$a_{max} = k\delta_{eq}^{n} \quad \text{(Eq 2)}$$

where k and n are constants. An analytical model proposed by Evans et al. (Ref 25) has shown that TGO thickness in a TBC can be expressed as

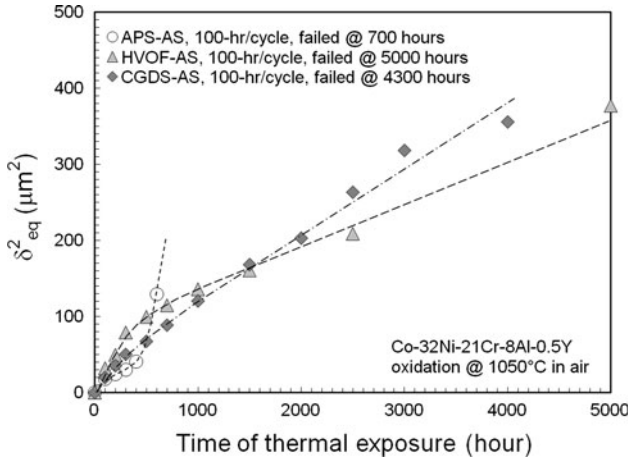

Fig. 6 The growth of TGOs in CoNiCrAlYs during thermal exposure. The TGO thickness of HVOF-CoNiCrAlY after 5000 h was measured from the remaining portion of the failed TBC sample

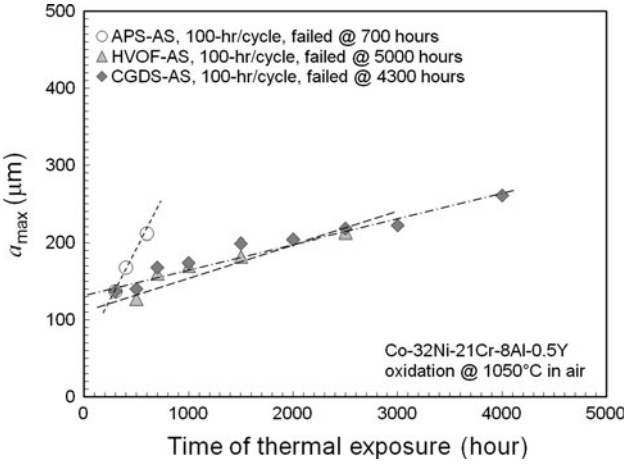

Fig. 7 The maximum crack length in the TBC as a function of the time of thermal exposure

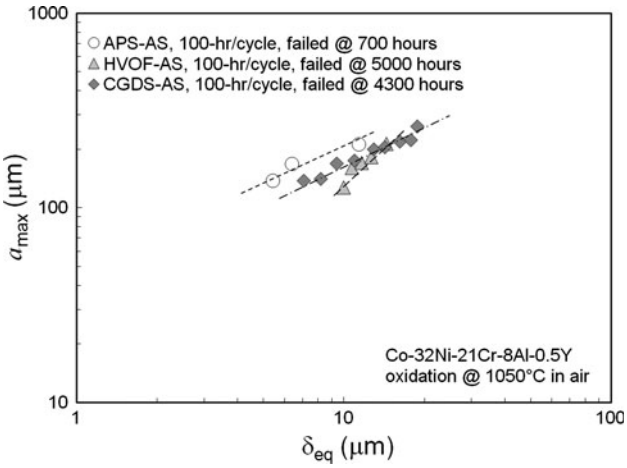

Fig. 8 The maximum crack length as a function of TGO thickness in TBCs with thermal- and cold-CoNiCrAlY bond coats

$$h = \frac{2\sqrt{\pi}(1-\upsilon^2)mK}{(m-1)RE}a^{\frac{3}{2}} \quad \text{(Eq 3)}$$

where h is the TGO thickness, a is the half crack length, R is the radius of the imperfection, m is the ratio of volume change, E is the Young's modulus of the TBC, υ is the Poisson's ratio, and K is the stress intensity factor.

Considering crack propagation during thermal cycling proceeds via discontinuity opening and coalescence in the ceramic near the TGO, $2R$ could be taken as the diameter of an individual splat, whereas $2a$ might be considered as the distance between two neighboring discontinuities. For crack propagation in a brittle material, when K is equal to K_{IC} (the fracture toughness), crack length and TGO thickness would therefore show the following relationship:

$$a = kh^{\frac{2}{3}} \quad \text{(Eq 4)}$$

where k is a constant.

However, the a_{max}-δ_{eq} relationship for APS-, HVOF-, and CGDS-CoNiCrAlY are quite different. This may be attributed to the different aluminum concentrations, which would affect the type and quantity of TGO, as well as the interface structure and residual stress state as produced by the different deposition techniques.

The CGDS-CoNiCrAlY appeared to have a lower TGO growth rate than the HVOF-CoNiCrAlY up to around 1000 h of thermal exposure at 1050 °C (Fig. 6); however, the TGO grew faster in CGDS-CoNiCrAlY afterwards, which agrees with the observation that preferable oxidation occurred at the open discontinuity between adjacent CoNiCrAlY powders near the ceramic/bond coat interface in the TBC with CGDS-CoNiCrAlY bond coat (Fig. 5). Therefore, optimization of the CGDS process, and/or a post-spraying surface treatment, such as shot-peening or laser ablating, may be necessary to remove the open discontinuities in the CGDS-CoNiCrAlY next to the ceramic/bond coat interface, to slow down the TGO growth.

It has been shown that the critical crack size for initiating TBC spallation is somehow related to the topcoat thickness (Ref 26). It is possible that TBCs with different topcoat thickness values would fail at different TGO thickness levels. As such, understanding of the relationship between crack length and TGO thickness, as well as the influence of spraying process on such a relationship, may be valuable for TBC life prediction. The nature of such a relationship merits further investigation via both numerical and experimental studies.

4. Conclusions

In this study, TGO growth behavior and cracking behavior were studied in TBC systems with APS-, HVOF-, and CGDS-CoNiCrAlY bond coats during thermal exposure.

It was observed that in APS-CoNiCrAlY the TGO exhibited a three-stage growth behavior, whereas in HVOF- and CGDS-CoNiCrAlYs, the growth of TGOs showed an instantaneous growth followed by a parabolic growth.

Cracking appeared to proceed predominantly via discontinuity opening and crack propagation in the ceramic layer near the TC/BC interface. Power-law relationships between the maximum crack length and the TGO thickness were observed in all three CoNiCrAlYs; however, it appeared that the spray process had an influence on the power-law relationship.

The TBCs with HVOF- and CGDS-CoNiCrAlY bond coats had an extended durability, compared to the TBC with APS-CoNiCrAlY bond coat. However, the durability of CGDS-CoNiCrAlY was not as good as the HVOF-CoNiCrAlY.

These results point to a potential advantage of using CGDS technique to produce TBC bond coats, for its significantly improved durability over the commercial air plasma spray bond coat, as well as its fast deposition rate and low deposition temperature. Furthermore, optimiza-

tion of the CGDS process as well as post-spraying surface treatment(s) deserves investigation in order for such CGDS technique to be employed in TBC bond coat production.

Acknowledgments

The authors thank Sylvain Bélanger and Frédéric Belval of the Industrial Materials Institute of NRC Canada for thermal spraying the TBC samples.

References

1. E.A.G. Shillington and D.R. Clarke, Spalling Failure of a Thermal Barrier Coating Associated with Aluminum Depletion in the Bond-Coat, *Acta Mater.*, 1999, **47**, p 1297-1305
2. A. Rabiei and A.G. Evans, Failure Mechanisms Associated with the Thermally Grown Oxide in Plasma-Sprayed Thermal Barrier Coatings, *Acta Mater.*, 2000, **48**, p 3963-3976
3. R.A. Miller and C.E. Lowell, Failure Mechanisms of Thermal Barrier Coatings Exposed to Elevated Temperatures, *Thin Solid Films*, 1982, **95**, p 265-273
4. A.G. Evans, D.R. Mumm, J.W. Hutchinson, G.H. Meier, and F.S. Pettit, Mechanisms Controlling the Durability of Thermal Barrier Coatings, *Prog. Mater. Sci.*, 2001, **46**, p 505-553
5. K.W. Schlichting, N.P. Padture, E.H. Jordan, and M. Gell, Failure Modes in Plasma-Sprayed Thermal Barrier Coatings, *Mater. Sci. Eng.*, 2003, **A342**, p 120-130
6. S.M. Meier, D.M. Nissley, and K.D. Sheffler, *Thermal Barrier Coating Life Prediction Model Development, ASME 91-GT-40*, International Gas Turbine and Aeroengine Congress and Exposition, Orlando, FL, 1991
7. Kh.G Schmitt-Thomas and M. Hertter, Improved Oxidation Resistance of Thermal Barrier Coatings, *Surf. Coat. Technol.*, 1999, **120-121**, p 84-88
8. W.R. Chen, X. Wu, B.R. Marple, D.R. Nagy, and P.C. Patnaik, TGO Growth Behaviour in TBCs with APS and HVOF Bond Coats, *Surf. Coat. Technol.*, 2008, **202**, p 2677-2683
9. W.R. Chen, X. Wu, B.R. Marple, R.S. Lima, and P.C. Patnaik, Pre-oxidation and TGO Growth Behaviour of an Air-Plasma-Sprayed Thermal Barrier Coating, *Surf. Coat. Technol.*, 2008, **202**, p 3787-3796
10. W.R. Chen, R. Archer, X. Huang, and B.R. Marple, TGO Growth and Crack Propagation in a Thermal Barrier Coating, *J. Therm. Spray Tech.*, 2008, **17**, p 858-864
11. W.R. Chen, X. Wu, B.R. Marple, X. Huang, and P.C. Patnaik, Cracking Behaviour of an Air-Plasma-Sprayed Thermal Barrier Coating, GT2009-59135, *Proceedings of ASME Turbo Expo 2009: Power for Land, Sea and Air*, Orlando, Florida, USA, June 8-12, 2009
12. P. Richer, B. Jodoin, E. Sansoucy, L. Ajdelsztajn, and G.E. Kim, Properties of Cold Spray Nickel Based Coatings, *Proceedings of the 2006 International Thermal Spray Conference*, Seattle, Washington, USA, May 15-18, 2006
13. T. Ichikawa, K. Sakaguchi, K. Ogawa, T. Shoji, S. Barradas, M. Jeandin, and M. Boustie, Deposition Mechanisms of Cold Gas Dynamic Sprayed MCrAlY Coatings, *Thermal Spray 2007: Global Coating Solutions*, p 54-59
14. Q. Zhang, C. Li, C. Li, G. Yang, and S. Lui, Study of Oxidation Behavior of Nanostructured NiCrAlY Bond Coatings Deposited by Cold Spraying, *Surf. Coat. Technol.*, 2008, **202**, p 3378-3384
15. Q. Zhang, C. Li, Y. Li, S. Zhang, X. Wang, G. Yang, and C. Li, Thermal Failure of Nanostructured Thermal Barrier Coatings with Cold-Sprayed Nanostructured NiCrAlY Bond Coat, *J. Therm. Spray Tech.*, 2008, **17**, p 838-845
16. F. Raletz, G. Ezo'o, M. Vardelle, and M. Ducos, Characterization of Cold-Sprayed Nickel-Base Coatings, *Thermal Spray 2004: Advances in Technology and Application*, ASM International, Osaka, Japan, May 10-12, 2004, p 323-328
17. Y. Ichikawa, K. Ogawa, M. Nivard, L. Berthe, M. Boustie, M. Ducos, S. Barradas, and M. Jeandin, Adhesion Study of Cold-Sprayed CoNiCrAlY-Mo Coating of Inconel 625 using the Laser Shock Adhesion Test (LASAT), *Mater. Sci. Forum 2*, 2007, **539-543**, p 1086-1091
18. P. Richer, A. Zúñiga, M. Yandouzi, and B. Jodoin, CoNiCrAlY Microstructural Changes Induced During Cold Gas Dynamic Spraying, *Surf. Coat. Technol.*, 2008, **203**, p 364-371
19. Y. Li, C.-J. Li, Q. Zhang, G.-J. Yang, and C.-X. Li, Influence of TGO Composition on the Thermal Shock Lifetime of Thermal Barrier Coatings with Cold-Sprayed MCrAlY Bond Coat, *J. Therm. Spray Tech.*, 2010, **19**, p 168-177
20. P. Richer, M. Yandouzi, L. Beauvais, and B. Jodoin, Oxidation Behaviour of CoNiCrAlY Bond Coats Produced by Plasma, HVOF and Cold Gas Dynamic Spraying, *Surf. Coat. Technol.*, 2010, **204**, p 3962-3974
21. W.R. Chen, X. Wu, B.R. Marple, and P.C. Patnaik, The Growth and Influence of Thermally Grown Oxide in a Thermal Barrier Coating, *Surf. Coat. Technol.*, 2006, **201**, p 1074-1079
22. J.A. Haynes, M.K. Ferber, W.D. Porter, and E.D. Rigney, Characterization of Alumina Scales Formed During Isothermal and Cyclic Oxidation of Plasma-Sprayed TBC Systems at 1150°C, *Oxid. Met.*, 1999, **52**, p 31-76
23. W. Brandl, H.J. Grabke, D. Toma, and J. Krüger, The Oxidation Behaviour of Sprayed MCrAlY Coatings, *Surf. Coat. Technol.*, 1996, **86-87**, p 41-47
24. K.S. Chan and N.S. Cheruvu, Degradation Mechanism Characterization and Remaining Life Prediction for NiCoCrAlY Coatings, GT2004-53383, *Proceedings of ASME Turbo Expo 2004, Power for Land, Sea, and Air*, Vienna, Austria, 2004
25. A.G. Evans, M.Y. He, and J.W. Hutchinson, Mechanics-Based Scaling Laws for the Durability of Thermal Barrier Coatings, *Prog. Mater. Sci.*, 2001, **46**, p 249-271
26. D. Zhu, S.R. Choi, and R.A. Miller, Development and Thermal Fatigue Testing of Ceramic Thermal Barrier Coatings, *Surf. Coat. Technol.*, 2004, **188-189**, p 146-152